Molecular Therapy
Nucleic Acids
Original Article

MicroRNA-212-5p, an anti-proliferative miRNA, attenuates hypoxia and sugen/hypoxia-induced pulmonary hypertension in rodents

Tianji Chen,[1] Miranda R. Sun,[1,7] Qiyuan Zhou,[1] Alyssa M. Guzman,[1] Ramaswamy Ramchandran,[1] Jiwang Chen,[2,3] Dustin R. Fraidenburg,[3] Balaji Ganesh,[4] Mark Maienschein-Cline,[5] Karl Obrietan,[6] and J. Usha Raj[1]

[1]Department of Pediatrics, College of Medicine, University of Illinois at Chicago, Chicago, IL 60612, USA; [2]Cardiovascular Research Center, University of Illinois at Chicago, Chicago, IL 60612, USA; [3]Department of Medicine, Division of Pulmonary, Critical Care, Sleep and Allergy, University of Illinois at Chicago, Chicago, IL 60612, USA; [4]Flow Cytometry Core, University of Illinois at Chicago, Chicago, IL 60612, USA; [5]Research Informatics Core, University of Illinois at Chicago, Chicago, IL 60612, USA; [6]Department of Neuroscience, Ohio State University, Columbus, OH 43210, USA

MicroRNAs (miRNA, miR-) play important roles in disease development. In this study, we identified an anti-proliferative miRNA, miR-212-5p, that is induced in pulmonary artery smooth muscle cells (PASMCs) and lungs of pulmonary hypertension (PH) patients and rodents with experimental PH. We found that smooth muscle cell (SMC)-specific knockout of miR-212-5p exacerbated hypoxia-induced pulmonary vascular remodeling and PH in mice, suggesting that miR-212-5p may be upregulated in PASMCs to act as an endogenous inhibitor of PH, possibly by suppressing PASMC proliferation. Extracellular vesicles (EVs) have been shown recently to be promising drug delivery tools for disease treatment. We generated endothelium-derived EVs with an enriched miR-212-5p load, 212-eEVs, and found that they significantly attenuated hypoxia-induced PH in mice and Sugen/hypoxia-induced severe PH in rats, providing proof of concept that engineered endothelium-derived EVs can be used to deliver miRNA into lungs for treatment of severe PH.

INTRODUCTION

Pulmonary hypertension (PH) is a disease characterized by a progressive increase in pulmonary vascular resistance, right ventricular failure, and ultimately death of patients.[1,2] Although the etiology is complex, a hallmark of PH is abnormal vascular wall remodeling associated with excessive proliferation of pulmonary artery smooth muscle cells (PASMCs).

MicroRNAs (miRNAs) are a class of endogenous small noncoding RNAs that are evolutionarily conserved[3–6] and have been reported to be involved in the pathogenesis of diseases, including PH.[7–11] We have previously reported that miR-17–92 plays a role in PH and that knockout of miR-17–92 in smooth muscle cells (SMCs) attenuated hypoxia-induced PH in mice.[12] However, the role of miRNA in PH needs to be studied further. We recently identified several miRNAs that are upregulated in mouse pulmonary vascular cells in hypoxia or lungs of mice with hypoxia-induced PH. Among these miRNAs, we found that miR-212-5p was the most powerful "anti-proliferative" miRNA in mouse PASMCs (mPASMCs).[13] In this study, we demonstrated that miR-212-5p significantly suppresses human PASMC proliferation *in vitro* and attenuates PH in mice and rats, offering a novel potential target for PH treatment.

Extracellular vesicles (EVs) are a heterogeneous family of membrane-limited vesicles originating from the endosome or plasma membrane.[14] Recent studies show that EV-mediated intercellular communications are evolutionarily conserved,[15] and their innate biocompatibility, capacity to deliver different types of cargo, and ability to target specific cells make them especially suitable as vehicles for drug delivery.[16–22] In this study, we loaded pulmonary vascular endothelial cell (PVEC)-derived EVs with miR-212-5p and provided the first proof of concept that engineered endothelium-derived EVs can be a powerful and promising tool for treatment of severe PH.

RESULTS

Expression of miR-212-5p was upregulated in PASMCs and lungs of PH patients and rodents with PH

We measured expression of miR-212-5p in PASMCs isolated from control donors and human PH patients[12] by qPCR analysis and found that miR-212-5p was significantly upregulated in PASMCs of PH patients (Figure 1A). Similarly, miR-212-5p was also significantly upregulated in PASMCs isolated from mice with hypoxia-induced PH (Figure 1B). We collected whole lungs of mice exposed to room air or hypoxia (10% O_2) for 1, 2, or 3 weeks and found that

Received 12 October 2021; accepted 15 June 2022;
https://doi.org/10.1016/j.omtn.2022.06.008.

[7]Present address: School of Veterinary Medicine, University of Wisconsin-Madison, Madison, WI 53706, USA

Correspondence: Tianji Chen, Department of Pediatrics, College of Medicine, University of Illinois at Chicago, Chicago, IL 60612, USA.
E-mail: tianjic@uic.edu
Correspondence: J Usha Raj, Department of Pediatrics, College of Medicine, University of Illinois at Chicago, Chicago, IL 60612, USA.
E-mail: usharaj@uic.edu

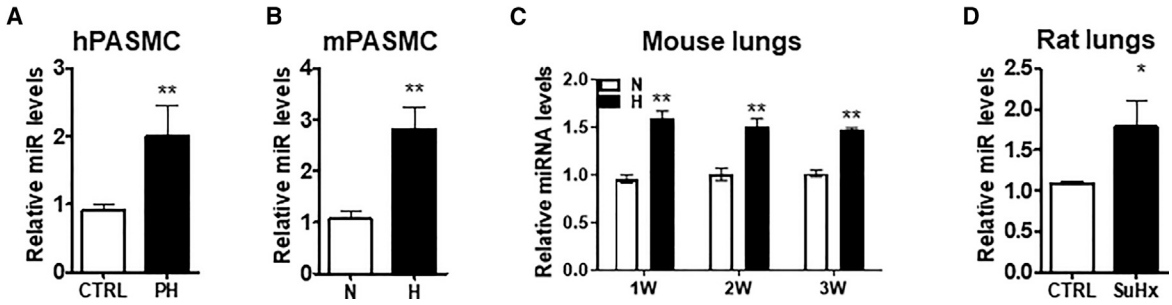

Figure 1. Expression of miR-212-5p is induced in PASMCs and the lung of PH subjects

Expression of miR-212-5p was measured by qRT-PCR analysis in the following samples. (A) PASMCs of human PH patients (n = 4) or normal donors (control, n = 9). (B) PASMCs isolated from control mice (N, exposed to room air, n = 8) or mice with hypoxia-induced PH (H, 10% O_2, 3 weeks, n = 7). (C) Lungs of control mice (N, exposed to room air, n = 5 for each time point) or mice exposed to hypoxia for 1, 2, or 3 weeks (H, 10% O_2, n = 5 for each time point). (D) Lungs of control rats (CTRL, given DMSO and stayed in room air, n = 6) or rats with Sugen/hypoxia-induced severe PH (SuHx, n = 5). Data are presented as mean ± SEM. * or **, versus CTRL or N. *p < 0.05, **p < 0.01.

miR-212-5p was significantly upregulated in mouse lungs in hypoxia at 1, 2, and 3 weeks (Figure 1C). We also found that miR-212-5p was significantly upregulated in the lungs of rats with Sugen5416/hypoxia-induced severe PH (Figure 1D). These data suggest a potential role for miR-212-5p in PH.

miR-212-5p is an "anti-proliferative" miRNA in PASMC

To investigate the role of miR-212-5p in PASMCs and PH, we first inhibited endogenous miR-212-5p in normal human PASMCs using miR-212-5p antagonist (Anti-miR-212-5p). Normal PASMCs transfected with negative control miR inhibitor (Anti-Neg) served as controls, and their proliferation level was set as 1. Using BrdU incorporation assay, we found that inhibition of endogenous miR-212-5p induced PASMC proliferation *in vitro* in room air (Figure 2A), suggesting that miR-212-5p inhibits PASMC proliferation *in vitro*.

Then, we transfected normal human PASMCs with miR-212-5p or negative control miR mimic and then exposed the cells to room air or hypoxia (1% O_2) for 24 h. We found that miR-212-5p significantly suppressed PASMC proliferation in both room air and hypoxia (Figure 2B). We also infected PASMCs with adenoviral particles that express exogenous miR-212-5p (Ad-miR212) or control adenoviral particles (Ad-Ctrl) and found that overexpression of miR-212-5p significantly suppressed PASMC growth, as shown by cell counting result at days 3 and 5 after adenoviral particle infection (Figure 2C). We also incubated these cells with platelet-derived growth factor (PDGF)-BB for stimulation of cell growth and found that overexpression of miR-212-5p significantly suppressed both basal proliferation level and PDGF-BB stimulated proliferation in PASMCs, as shown by immunofluorescence staining of proliferation marker protein Ki-67 (Figure S1). Similarly, miR-212-5p also suppressed proliferation of PASMCs isolated from PH patients (Figure 2D). Our data suggest that miR-212-5p is an anti-proliferative miRNA in PASMCs.

MiR-212-5p acts as an endogenous inhibitor of PH

To investigate if the endogenous miR-212-5p in PASMCs plays a role in PH, we generated a strain of SMC-specific knockout miR-212-5p mice by crossbreeding the miR-212-5p flox/flox mice [212 fl/fl[23,24]] with SM22αCre mice (sm-212$^{-/-}$, Figure 3A). Mouse genotype was validated by PCR analysis (Figure 3B). PASMCs were isolated, as described before,[12] from sm-212$^{-/-}$ mice and their 212 fl/fl littermates. miR-212-5p knockdown efficiency in SMCs was confirmed by qPCR analysis (Figure 3C). We exposed these sm-212$^{-/-}$ mice and their 212 fl/fl littermates to room air or hypoxia (10% O_2) for 3 weeks and found that SMC-specific knockout of miR-212 significantly exacerbated hypoxia-induced RVSP elevation (Figure 3D), right ventricular (RV) hypertrophy (Fulton's index, Figure 3E), and pulmonary vessel wall thickening (Figures 3F and 3G) in mice. These results suggest a protective role of the endogenous miR-212-5p in SMCs in PH.

We also injected C57BL/6 wild-type mice with miR-212-5p inhibitor (Anti-miR212) through the tail vein twice a week for 2 weeks (mice injected with negative control miRNA inhibitor [Anti-Neg] served as controls) while mice were in room air (N) or hypoxia (10% O_2, H) (Figure S2A). Then, PH indices were measured and lungs collected for study. Using *in situ* hybridization (ISH), we observed a much weaker staining of miR-212-5p in the lungs, including pulmonary vessels, of mice that received miR-212-5p inhibitor (versus mice given Anti-Neg) (Figure S2B). Using qPCR analyses, we also found a significantly lower level of miR-212-5p in lungs of mice given miR-212-5p inhibitor (Figure S2C), attesting to the efficiency of miR-212-5p inhibition in the lung. Inhibition of miR-212-5p increased RVSP both in room air and hypoxia (Figure S2D) and further increased RV hypertrophy in hypoxia (Figure S2E). Increase in pulmonary vascular wall remodeling did not reach significance (Figure S2F and S2G). These results suggest that inhibition of endogenous miR-212-5p using miRNA inhibitors exacerbated hypoxia-induced PH in mice, further confirming a protective role of endogenous miR-212-5p in PH.

Exogenous miR-212-5p attenuates hypoxia-induced PH in mice

Because miR-212-5p is a powerful anti-proliferative miRNA in PASMCs, we investigated if administration of exogenous miR-212-5p can inhibit hypoxia-induced PH in mice. We injected

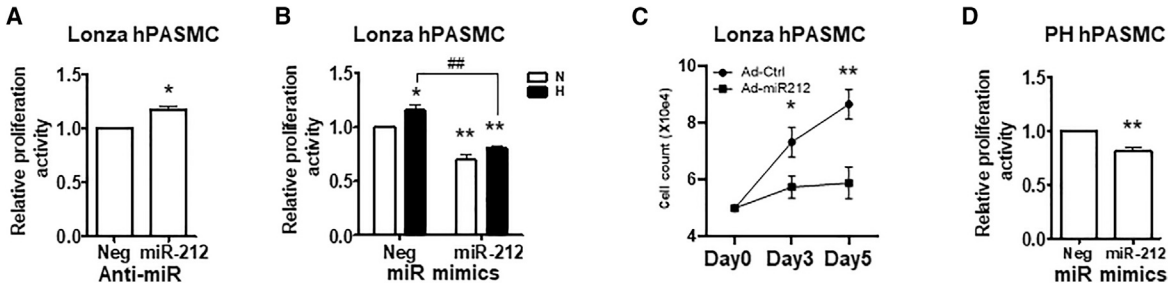

Figure 2. MiR-212-5p is an "anti-proliferative" miRNA in PASMC

(A) Normal human PASMCs (hPASMCs, Lonza) were transfected with miR-212-5p or negative control miR inhibitor (Anti-miR-212 versus Anti-Neg). BrdU incorporation assay was performed. Proliferation level of PASMCs transfected with negative control miR inhibitor (Anti-Neg) was set as 1 and served as controls. Proliferation level of PASMCs transfected with miR-212-5p inhibitor (Anti-miR-212) was compared with that of control cells. Inhibition of miR-212-5p induced PASMC proliferation *in vitro* in room air. (B) Normal hPASMC (Lonza) were transfected with miR-212-5p or negative control miR mimic and then exposed to room air (N) or hypoxia (H, 1% O_2) for 24 h. BrdU incorporation assay was performed to determine the relative proliferation level of these cells. Proliferation level of PASMCs transfected with negative control miR mimic (Neg mimic) and exposed to room air was set as 1 and served as controls. Proliferation levels of PASMCs in other groups were compared with that of control cells. miR-212-5p mimic significantly suppressed PASMC proliferation in both room air and hypoxia. (C) Normal hPASMCs (Lonza) were infected with adenoviral particles that express miR-212-5p (Ad-miR212, 100 PFUs/cell) or control adenoviral particles (Ad-Ctrl, 100 PFUs/cell) on day 1. Then cells were collected for cell counting on day 3 and 5, respectively. Overexpression of miR-212-5p significantly suppressed cell growth in room air. (D) Human PASMCs of PH patient (PH hPASMCs) were transfected with miR-212-5p or negative control miR mimic. BrdU incorporation assay was performed and relative cell proliferation level was compared, as described above. miR-212-5p mimic also significantly suppressed proliferation of PH hPASMCs. Data are presented as mean ± SEM. * or ** versus room air Anti-Neg, Neg mimic control, or Ad-Ctrl, respectively; ## versus hypoxic Neg mimic control. *p < 0.05, ** or ##p < 0.01.

C57BL/6 wild-type mice with negative control (Neg) or miR-212-5p mimic via tail vein twice per week for 3 weeks, while mice were exposed to room air (N) or hypoxia (10% O_2, H) (Figure 4A). Lungs were collected at the end of the study and stained with miR-212-5p probes. Moderately increased miR-212-5p staining was observed in pulmonary vessel walls and lungs of mice given miR-212-5p mimic (Figures 4B and 4C). Administration of miR-212-5p mimic partially and significantly attenuated hypoxia-induced RVSP elevation (Figure 4D) and pulmonary vessel wall remodeling (Figures 4F and 4G), while hypoxia-induced RV hypertrophy (Figure 4E) was not changed.

Exogenous miR-212-5p attenuates Sugen5416/hypoxia-induced severe PH in rats

To determine if exogenous miR-212-5p can reverse established PH in rats, we first injected 6-7-week-old Sprague-Dawley rats with Sugen5416 (20 mg/kg body weight [BW], subcutaneously [s.c.]) and exposed them to hypoxia (H, 10% O_2) for 3 weeks, followed by 2 weeks' room air exposure to induce severe PH. Then, we started weekly intratracheal (i.t.) administration of adenoviral particle (Ad-miR-212-5p or Ad-Ctrl) into rats while they stayed in room air for another 3 weeks (Figure 5A). Results of ISH staining using a miR-212-5p probe showed that miR-212-5p staining was significantly stronger in both airway and pulmonary vessels of lungs of rats given Ad-miR-212-5p (Figure 5B). The amount of miR-212-5p in the whole lung was also increased, as determined by qPCR analysis (Figure 5C). We dissected pulmonary vessels and stripped off the outer adventitial coat to collect mainly the muscle coat for qPCR analysis and found that miR-212-5p level was significantly increased in pulmonary vessel muscle coat of rats receiving Ad-miR-212-5p (Figure 5D), further confirming that exogenous miR-212-5p was successfully delivered into the pulmonary vessel wall by i.t. delivery. PH indices were significantly reduced by administration of exogenous miR-212-5p: there was a reduction in Sugen5416/hypoxia (SuHx)-induced increase in RVSP (Figure 5E), RV hypertrophy (Figure 5F), and pulmonary vessel wall remodeling (Figures 5G and 5H) in rats.

Generation of engineered mPVEC-derived EVs with increased levels of miR-212-5p

Recent studies suggest that extracellular vesicles (EVs) are naturally occurring cargo delivery agents, which can be used as vehicles for drug delivery. Their innate biocompatibility, capacity to deliver different types of cargo, and ability to target specific cells make them especially suitable for this task.[16–22] In this study, we engineered EVs (eEVs) derived from PVECs to contain excess exogenous miR-212-5p, for use in the treatment of established PH *in vivo*. We infected mPVECs with the XMIRXP-control or XMIRXP-miR-212 lentiviral particles that can express miR-212-5p and then collected EVs from the conditioned medium (Figure S3A). We designated these EVs as Ctrl- and 212-eEVs, respectively, and confirmed the selective loading of miR-212-5p in 212-eEVs by qPCR analysis (Figures S3B and S3C). Our results showed that isolated eEVs expressed specific endothelial cell marker proteins CD31 and CD144 (Figure S3D), confirming their endothelial origin.[14] These eEVs did not express exosome markers heat shock protein 70 kDa (HSP70)[25,26] and expressed very low levels of CD81 (Figure S3D), confirming that the eEVs we collected in this study were mainly microvesicles (MVs), but not exosomes. These results are consistent with our previous findings that EVs (not engineered) collected by ultracentrifugation at 20,500 g for 1 h are mostly MVs, not exosomes.[13]

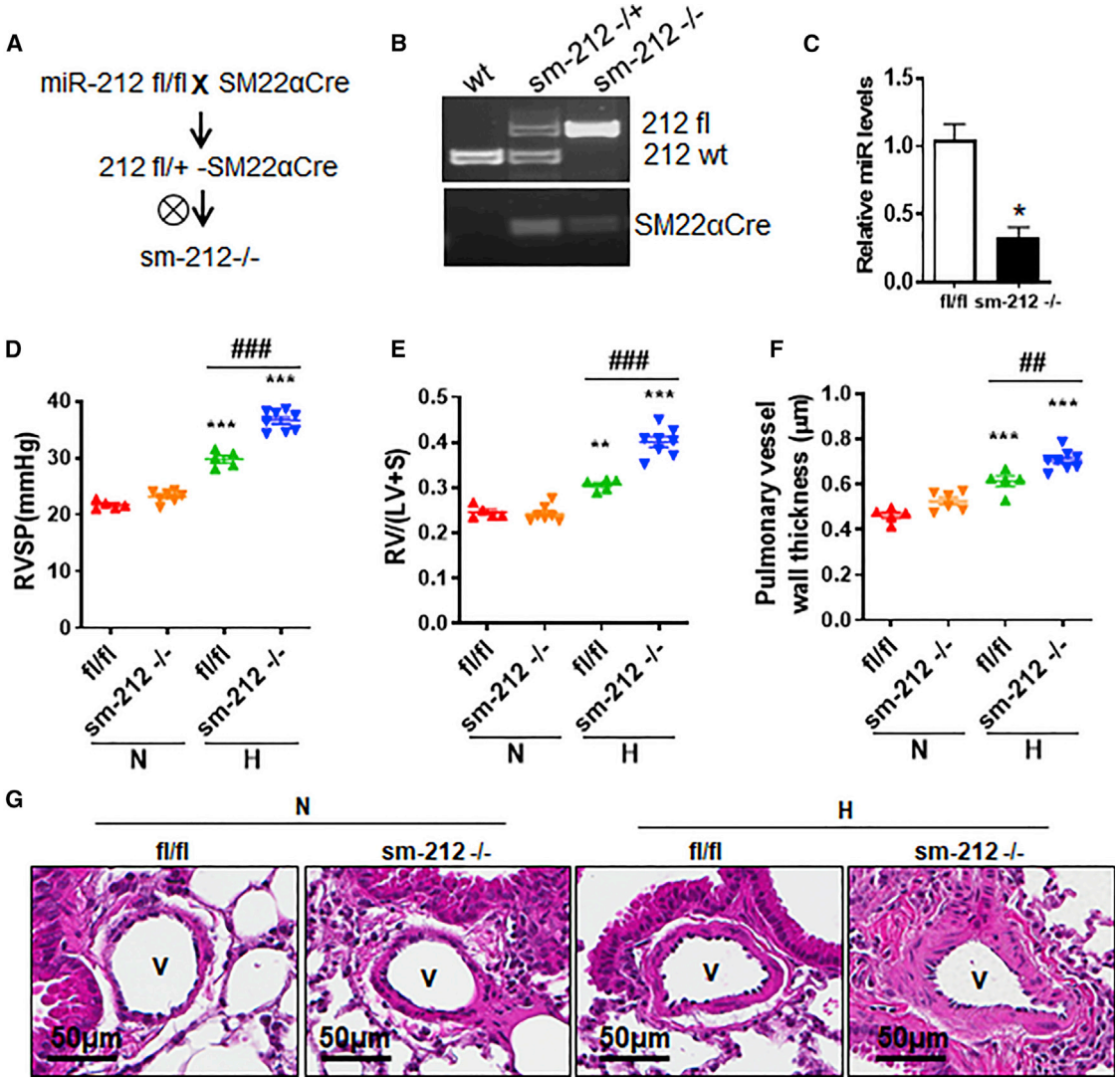

Figure 3. SMC-specific knockout of miR-212 significantly exacerbates hypoxia-induced PH in mice

(A) The strategy to generate smooth muscle cell (SMC)-specific miR-212 knockout mice and mouse genotyping (B). (C) The expression levels of miR-212-5p in freshly isolated mouse PASMCs (mPASMCs) from sm-212$^{-/-}$ mice (n = 4) and their 212-fl/fl littermates (n = 4). sm-212$^{-/-}$ and their 212-fl/fl littermates were exposed to room air or hypoxia (10% O_2) for 3 weeks and then PH indices were measured. SMC-specific knockout of miR-212 significantly exacerbated hypoxia-induced RVSP elevation (D), RV hypertrophy (E), and pulmonary vessel wall thickening (F–G). V: vessels. Data are presented as mean ± SEM. *, **, or *** versus fl/fl control in room air; ## or ### versus fl/fl control in hypoxia; *p < 0.05, ** or ##p < 0.01, ###p < 0.001.

212-eEVs inhibit hypoxia-induced PASMC proliferation in culture

We incubated mPASMCs with Ctrl- or 212-eEVs and exposed the cells to room air (N) or hypoxia (H, 1% O_2) for 24 h. Using BrdU incorporation assay, we found that 212-eEVs decreased hypoxia-induced PASMC proliferation (Figure S3E), suggesting that miRNA can be loaded into mPVEC-derived EVs and be functional.

eEVs given intratracheally into mice can enter pulmonary blood vessels

Next, we labeled Ctrl-eEVs with ExoGlow-Vivo EV Labeling Kit (near-infrared [near-IR]) and instilled labeled eEVs into mice via the trachea. Control mice received Dulbecco's phosphate-buffered saline (DPBS). Lungs were collected 10 min, 1 h, 3 h, and 24 h later for frozen tissue section and stained for α-smooth muscle actin (α-SMA) and DAPI. We first identified a vessel about 100–150 μm in diameter in the 10 min lung section and obtained images with excitation filter of 488 nm (for α-SMA), 740 nm (for near-IR-labeled EV), and 387 nm (for DAPI). We could visualize eEVs within the pulmonary vessel wall (Figure S4A), indicating that some of the eEVs did enter the pulmonary vessel wall. We also identified labeled eEVs in the lung (both airways and vessels) 1 and 3 h after eEV delivery but could not detect labeled eEVs in pulmonary vessels 24 h after delivery

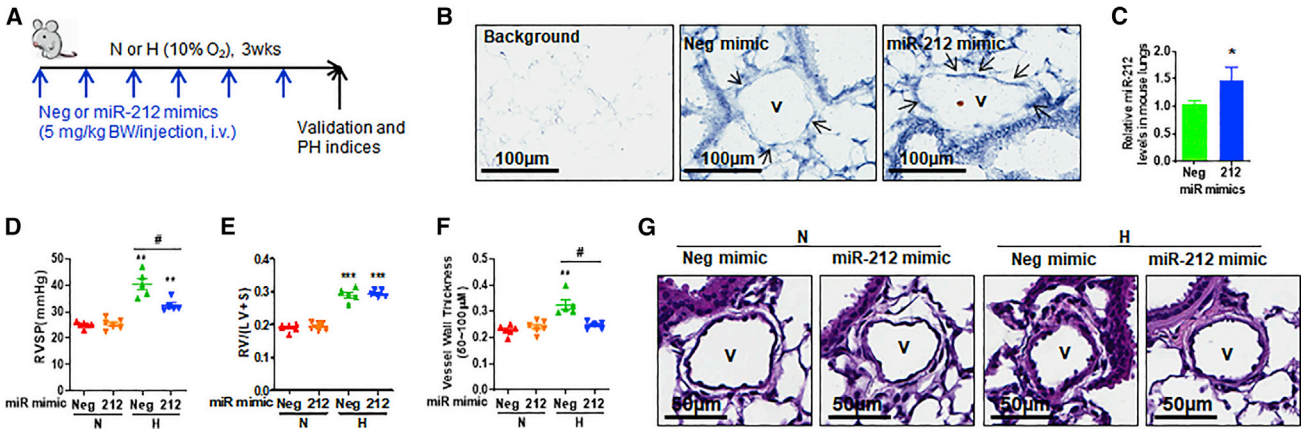

Figure 4. miR-212-5p attenuates hypoxia-induced PH in mice

(A) Experimental design: 6-8-week-old C57BL/6 mice were injected with miR mimic via tail vein (5 mg/kg BW/injection, twice a week) and exposed to room air (N) or hypoxia (H, 10% O_2) for 3 weeks. At the end of the study, moderately increased miR-212-5p staining was observed in pulmonary vessel walls as pointed by the arrows (B, ISH, arrows point to miR-212-5p staining). MiR-212-5p levels was also increased in the lung (C, qRT-PCR analysis). Our results show that administration of miR-212-5p mimic significantly attenuated hypoxia-induced RVSP elevation (D) and pulmonary vessel wall remodeling (F–G), while RV hypertrophy (E) was not changed. V: vessels. Data are presented as mean ± SEM in C–F. ** or *** compared with N-Neg mimic group; # compared with H-Neg mimic group. #$p < 0.05$; **$p < 0.01$; ***$p < 0.001$. N = 5–6.

(Figure S4B), possibly due to a diffusion of the eEV signal by 24 h after eEV administration. Imaging result with z axes showed that eEVs were taken up into SMCs in the pulmonary vessel wall, rather than just being attached to them (Figure S4B and Video S1). We were also able to deliver the nonmammalian Cel-miR-39 successfully into the pulmonary vessel wall via PVEC-derived eEVs, further confirming that PVEC-eEVs can be used to deliver exogenous miRNAs into PASMCs via i.t. administration (Figure S5).

212-eEVs attenuate hypoxia-induced PH in mice

We exposed C57BL/6 wild-type mice to hypoxia (10% O_2) for 2 weeks to establish PH and then gave eEVs, i.t., twice a week for 2 weeks, while mice were still in hypoxia (Figure 6A). Terminally, we found significantly stronger staining of miR-212-5p in the lungs, including the vessels, of mice given 212-eEVs (Figure 6B). Using qPCR analyses, we confirmed that miR-212-5p level was increased in lungs of mice that received 212-eEVs (Figure 6C). We measured PH indices and found that 212-eEVs significantly attenuated hypoxia-induced RVSP increase (Figure 6D), RV hypertrophy (Figure 6E), and pulmonary vessel wall remodeling (Figures 6F and 6G), suggesting that 212-eEVs attenuate hypoxia-induced PH.

rPVEC-derived 212-eEVs ameliorate SuHx-induced severe PH in rats

We generated rat PVEC-derived Ctrl- or 212-eEVs following a similar procedure to that in Figure S3A, using rat PVECs. Increased miR-212-5p level in eEVs was confirmed by qPCR analysis (data not shown). The 6-7-week-old Sprague-Dawley rats were injected with one dose of Sugen5416 (20 mg/kg BW, s.c.) and exposed to hypoxia (H, 10% O_2) for 3 weeks, followed by 2 weeks room air exposure to induce severe PH. Then, Ctrl- or 212-eEVs were delivered into these rats via the trachea, weekly for 3 weeks (Figure 7A). Rat lungs were collected at the end of the study for sectioning and ISH staining with a miR-212-5p probe. We found significantly stronger staining of miR-212-5p in the lung, including the vessels, of rats receiving 212-eEVs (Figure 7B). We also measured miR-212-5p levels in the lung, heart, kidney, spleen, and liver of these rats and confirmed that miR-212-5p levels were significantly induced in only the lungs of rats receiving 212-eEVs (Figure 7C), but not in other organs (Figure S6). We measured PH indices and found that 212-eEVs significantly attenuated SuHx-induced RVSP elevation (Figure 7D), RV hypertrophy (Figure 7E), and pulmonary vessel wall remodeling (Figures 7F and 7G) in rats, suggesting that 212-eEVs significantly ameliorated established severe PH in rats.

DISCUSSION

In this study, we demonstrated that miR-212-5p level is upregulated in PASMCs and lungs in human PH patients and rodent models of PH, suggesting a role for miR-212-5p in the pathogenesis of PH. To investigate the role of miR-212-5p *in vivo*, we generated a strain of SMC-specific miR-212 knockout mice. We found that SMC-specific knockout of miR-212-5p significantly exacerbated hypoxia-induced pulmonary vessel wall thickening and PH in mice, suggesting a protective role of SMC-specific miR-212-5p in pulmonary vascular remodeling and PH. We also provided the first evidence that administration of exogenous miR-212-5p attenuates both chronic hypoxia-induced PH in mice and Sugen/hypoxia-induced severe PH in rats. Our findings indicate that endogenous miR-212-5p is induced during the pathogenesis of PH, to act as an adaptive and protective agent to mitigate the severity of PH *in vivo*. This is in line with our previous finding that while pathogenic mechanisms contribute to the pathogenesis of PH, endogenous protective mechanisms are also activated to moderate the severity of the disease.[12] While the endogenous induction of miR-212-5p is insufficient to completely prevent or reverse

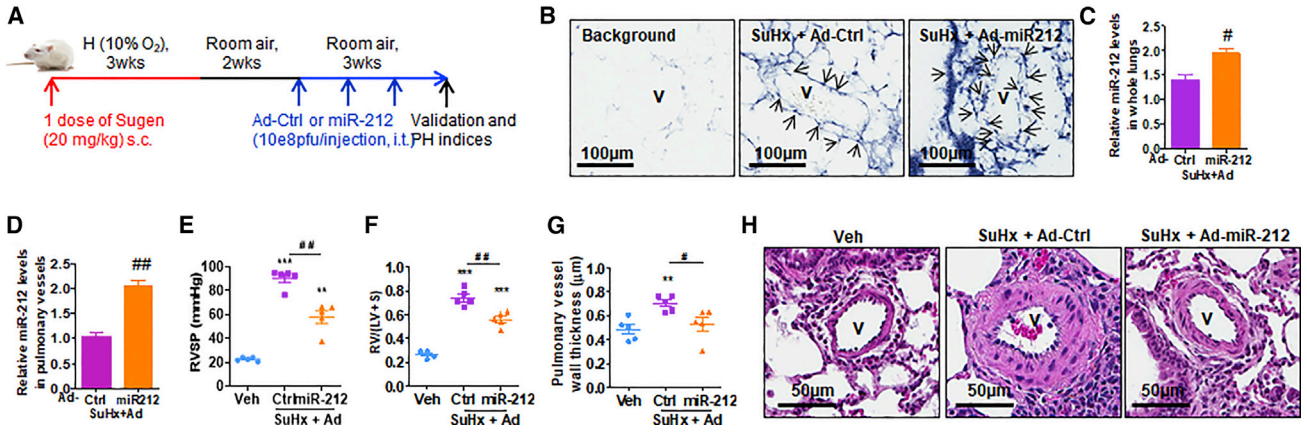

Figure 5. MiR-212-5p attenuates established severe PH in rats

(A) Experimental design: 6-7-week-old Sprague-Dawley rats were given one dose of Sugen5416 (20 mg/kg BW, s.c.) and then exposed to hypoxia (H, 10% O_2) for 3 weeks, followed by 2 weeks in room air, to induce severe PH. Then, rats were given intratracheally (i.t.) Control adenoviral particles (Ad-Ctrl) or adenoviral particles expressing miR-212-5p (Ad-miR-212), weekly for 3 weeks, while they were in room air. Rats given DMSO and exposed to room air served as controls (Veh). At the end of the study, an increase in miR-212-5p in the lung was validated by *in situ* hybridization (ISH) with miR-212-5p probe (B, arrows point to miR-212-5p staining) and qRT-PCR analysis (C). Increase in miR-212-5p level in isolated pulmonary vessels was also validated by qRT-PCR analysis (D). Administration of Ad-miR-212 significantly attenuated SuHx-induced RVSP elevation (E), RV hypertrophy (F), and pulmonary vessel wall remodeling (G–H) in rats. V: vessels. Data are presented as mean ± SEM in C–G. ** or *** compared with DMSO (Veh) group; # or ## compared with Ad-Ctrl group. #p < 0.05; ** or ##p < 0.01; ***p < 0.001. SuHx: Sugen5416/hypoxia. N = 5.

the development of PH, administration of exogenous level of miR-212-5p significantly ameliorates hypoxia-induced PH in mice and Sugen/hypoxia-induced PH in rats, suggesting that miR-212-5p could be a potential therapeutic target for PH treatment.

So far, only limited upstream regulators for miR-212-5p expression have been identified.[27–29] While a recent study showed that miR-212-5p was upregulated by hypoxia-inducible factor-1α (HIF-1α) in pancreatic cancer cells in hypoxia,[29] we do not know if HIF-1α mediates the upregulation of miR-212-5p in PASMCs in human PAH patients or rodents with PH, as the regulation of gene expression is always cell-type, tissue-type, and disease-background dependent. The cAMP-responsive transcription factor (CREB) has been recently identified as another transcriptional regulator for miR-212 in neuron cells, macrophages, or insulin-secreting β-cells.[27,28,30] Recent studies showed that an extracellular cyclic AMP (cAMP)/CREB signaling in pulmonary arteries (including both smooth muscle and endothelial cells on the vessels) is activated to mitigate the severity of pulmonary vascular remodeling and PH[31] and that SMC-specific knockout of CREB induced pulmonary vessel wall thickening and PH in mice.[32] These findings not only revealed a protective mechanism that is activated during the pathogenesis of PH, but also led to our speculation that miR-212-5p is upregulated by CREB in PASMCs to play the protective role in PH. Further studies with PASMCs are warranted to test our speculation.

EVs are currently being engineered to be powerful drug delivery vehicles[33] as well as to carry specific cargo for use as therapeutic agents in diseases. Kamerkar et al. have shown that exosomes can be engineered to carry small interfering RNA (siRNA) to specifically target Kras in pancreatic cancer.[17] EVs derived from mesenchymal stem cells (MSCs) have also been studied recently in PH. Aliotta et al. found that MSC-EV can attenuate the development of MCT-induced PH in mice.[34] In another study, Lee and colleagues demonstrated that MSC-derived exosomes exert a pleiotropic protective effect on the lung and inhibit vascular remodeling and hypoxic PH, with suppression on the STAT3/miR-17 level and induction of miR-204 level in the lung.[35] In this study, we have provided the first proof of concept that endothelium-derived EVs can be engineered to deliver exogenous miRNAs into the lung to treat PH, in both mouse and rat models of PH. We used EV-derived from PVECs in room air, since they had no effect on PASMC proliferation (data not shown).

eEVs were delivered via the trachea in our study, so that they can be specifically delivered into the lung, without off-target delivery into other organs. This is confirmed by our qPCR analysis showing that miR-212-5p levels are not induced in other organs (Figure S6). However, it is not surprising that eEVs administered via the trachea reach multiple cell types in the lung, including airway cells and vessel cells (Figure S4 and Video S1). While our data provided the first proof of concept that eEVs can be administered via the trachea to deliver therapeutic reagents into pulmonary vessels and PASMCs (instead of just attaching to PASMCs, Figure S4 and Video S1) for PH treatment, it is critical that EVs can be further engineered for tissue- or cell-type-specific delivery for future application of EVs in disease treatment.

Although our finding that SMC-specific knockout of miR-212 exacerbated hypoxia-induced pulmonary vascular remodeling and PH in mice supports our hypothesis about the protective role of miR-212, specifically in SMCs, it is worth noting that exogenous miR-212-5p (through adenoviral particles or eEVs) was delivered via the trachea

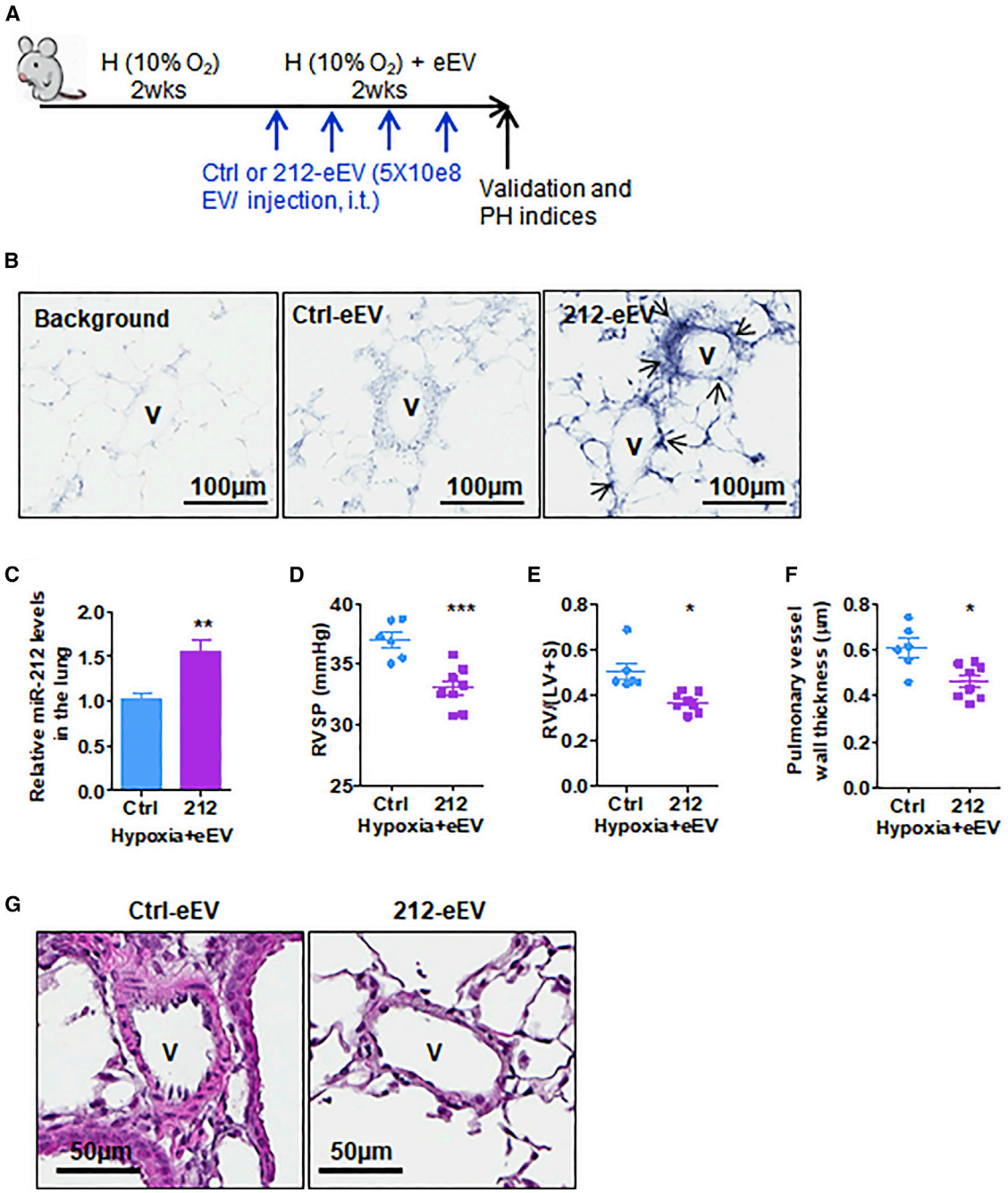

Figure 6. 212-eEVs ameliorate hypoxia-induced PH in mice

(A) Experimental design: 6-8-week-old C57BL/6 mice were exposed to hypoxia (H, 10% O_2) for 2 weeks to establish PH and then treated with 5 × 10e8 Ctrl- or 212-eEVs via the trachea, twice a week for 2 weeks while mice were still exposed to hypoxia. (B) Mouse lung sections were stained with a miR-212-5p probe (*in situ* hybridization, arrows point to miR-212-5p staining). miR-212-5p staining was significantly increased in lungs, including the vessels, in mice that received 212-eEVs. (C) miR-212-5p levels were measured by qPCR analysis and confirmed to be increased in lungs of mice that received 212-eEVs. (D–G) 212-eEVs significantly ameliorated hypoxia-induced RVSP elevation (D), RV hypertrophy (E), and pulmonary vessel wall remodeling (F–G). V: vessels. Data are presented as mean ± SEM in C–F. * or ** or *** compared with Ctrl-eEV-treated mice. *$p < 0.05$; **$p < 0.01$; ***$p < 0.001$. Ctrl-eEVs: n = 6; 212-eEVs: n = 8.

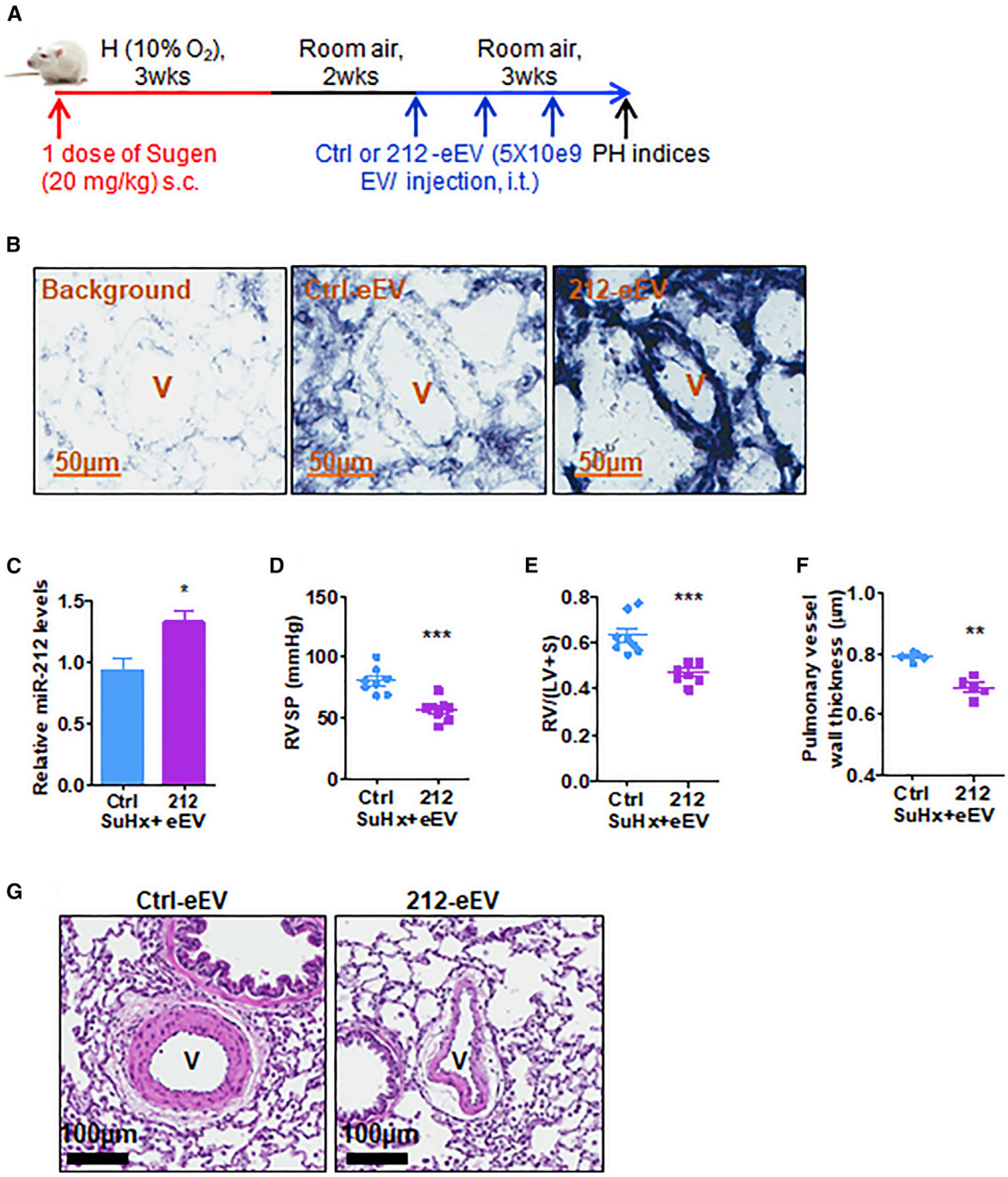

Figure 7. 212-eEVs ameliorate Sugen/hypoxia-induced severe PH in rats

(A) Experimental design: 6-7-week-old Sprague-Dawley rats were given one dose of Sugen5416 (20 mg/kg BW, s.c.) and then exposed to hypoxia (H, 10% O_2) for 3 weeks, followed by 2 weeks in room air to induce severe PH. Then rats were treated with 5 × 10e9 Ctrl- or 212-eEVs via the trachea, weekly for 3 weeks. (B) Rat lung sections were stained with a miR-212-5p probe (*in situ* hybridization, arrows point to miR-212-5p staining). miR-212-5p staining was significantly increased in lungs, including in the vessels, of rats that received 212-eEVs. (C) miR-212-5p levels were measured by qPCR analysis and confirmed to be increased in lungs of rats that received 212-eEVs. (D–G) Treatment with 212-eEVs significantly ameliorated Sugen/hypoxia (SuHx)-induced RVSP elevation (D), RV hypertrophy (E), and pulmonary vessel wall remodeling (F–G). V: vessels. Data are presented as mean ± SEM in C–F. * or ** compared with Ctrl-eEV-treated mice. **p < 0.001. N = 8.

and was not PASMC-specific in the present studies (Figures 5, 6, and 7). It is possible that miR-212-5p may also play a role in other cell types (like endothelial cells, etc.), which may also contribute to the attenuation of PH. Further studies are warranted to reveal the role of miR-212-5p in other cells types (like endothelial cells, etc.) in PH.

In summary, we have demonstrated the protective role of SMC-specific miR-212-5p in PH. Administration of exogenous miR-212-5p significantly attenuates PH in rodent models. We also provided the first proof of concept that engineered endothelium-derived EVs can be a powerful and promising therapeutic tool for treatment of severe PH. Further studies to find means of delivering the eEVs to their specific target, namely PASMCs, are warranted.

MATERIALS AND METHODS

Cell culture

Mouse pulmonary artery smooth muscle cells (mPASMCs) were isolated from mouse lungs, as we described previously,[12] and were maintained in SmGM-2 medium (Lonza, Walkersville, MD) containing 5% fetal bovine serum (FBS), growth factors, and 1% penicillin-streptomycin. We also isolated mPASMCs from mice exposed to 10% O_2 for 3 weeks and from mice exposed to room air for 3 weeks (controls). The purity of isolated PASMCs was confirmed by immunostaining of α-SMA (Figure S7).

Human pulmonary artery smooth muscle cells (hPASMCs) were purchased from Lonza. hPASMCs isolated from normal human lungs (donor lungs that could not be used) and from lungs of PH patients were provided by the Pulmonary Hypertension Breakthrough Initiative (PHBI). Patient or donor clinical information was described previously.[12] These cells were maintained in SmGM-2 medium containing FBS and growth factors (Lonza).[12] Use of these cells was approved by the University of Illinois at Chicago Institutional Review Board.

Mouse and rat pulmonary vascular endothelial cells (mPVECs and rPVECs) were purchased from Cell Biologics (Chicago, IL) and maintained in Endothelial Cell Medium containing 5% FBS, endothelial cell growth factors, and antibiotics (Cell Biologics).

All cells were maintained in a humidified incubator with a constant supply of 5% CO_2 at 37°C.

Engineering and isolation of extracellular vesicles

To generate engineered extracellular vesicles (eEVs) that can be used as a tool for miRNA delivery, we used an XMIRXPress Lentiviral system (System Biosciences, Palo Alto, CA) that contains a target sequence (GGAG)[36,37] in the 3′-end of miR-212-5p to direct the expressed miR-212-5p into EVs. We infected PVECs with the XMIRXP-miR-212 lentiviral particles and selected the cells using puromycin (1 μg/mL, Fisher Scientific) to generate stable XMIRXP-miR-212 PVEC cell lines. PVECs infected with XMIRXP-control lentivirus were used as control. Cells were cultured in room air for 24–48 h and EVs were collected from the supernatant (20,500 g), as described below. These EVs were designated as Ctrl- or 212-eEVs, respectively.

EV were isolated from cultured PVECs using a multi-step centrifugation method.[13,38–41] Briefly, after obtaining confluent monolayers of PVECs, the medium was refreshed with medium free of FBS or vesicles. Conditioned medium was collected and cell debris pre-cleared by centrifugation at 2,000 g for 15 min (min) at 4°C. The supernatant was centrifuged at 20,500 g for 1 h at 4°C. Pelleted vesicles were washed with ice-cold vesicle-free DPBS and pelleted again by centrifugation at 20,500 g for 1 h at 4°C. Finally, the pelleted vesicles were resuspended in vesicle-free DPBS. Collected vesicles were quantified using nanoparticle tracking analysis (NTA) technology with a NanoSight LM10 HS instrument (Malvern Instruments, Malvern, UK) at the Flow Cytometry Core of the University of Illinois at Chicago (UIC).

For characterization, collected eEVs were lysed in modified radioimmunoprecipitation assay buffer (mRIPA) buffer (50 mM Tris pH 7.4, 1% NP-40, 0.25% deoxycholate, 150 mmol/L NaCl, and protease inhibitors) and used for western blot analysis of PVECs or exosome markers, as we described before.[13] Briefly, 10 μg (for EV samples) or 30 μg (for PVEC samples) of protein lysate was separated by SDS-polyacrylamide gel electrophoresis and transferred to BA85 nitrocellulose membrane (Protran, Whatman, Dassel, Germany). Proteins were detected with SuperSignal West Pico or Femto chemiluminescent substrate (Thermo Scientific, Waltham, MA). The following primary antibodies were used: CD144 (Santa Cruz Biotechnology, Dallas, TX), CD31 (R&D Systems, Minneapolis, MN), HSP70 (System Biosciences), CD81 (System Biosciences), and α-Tubulin (Sigma-Aldrich).

Imaging of eEVs in the pulmonary vessel wall

eEVs were labeled with ExoGlow-Vivo Labeling Kit (near-IR dye, System Biosciences) and then instilled into mice through their trachea. Mouse lungs were collected for frozen tissue section and stained with α-SMA antibody at 10 min, 1 h, 3 h, and 24 h after eEV delivery. Lungs of control mice receiving DPBS were also studied. Near-IR dye-labeled eEVs were imaged using an Olympus IX81 inverted widefield microscope or a Leica Stellaris 8 laser scanning confocal microscope at the Integrated Light Microscopy Core Facility of the University of Chicago and analyzed using an Imaris X64 program.

RNA isolation and quantitative real-time reverse transcription PCR

Total RNA was isolated using a miRNeasy Mini Kit or miRNeasy Micro Kit (Qiagen, Valencia, CA) and treated with RNase-Free DNase I (Qiagen),[12] quantified with Nanodrop 2000 spectrophotometer (Thermo Scientific).

For quantitative real-time reverse transcriptase PCR (qRT-PCR) analysis of miRNA expression, a poly(A) tail was first added to the 3′-end of miRNAs using a Poly(A) Polymerase Tailing Kit (Epicentre Biotechnologies, Madison, WI). Poly(A) tailed-miRNAs were then reverse transcribed using M-MLV Reverse Transcriptase (Invitrogen, Grand Island, NY) with a poly(T) adaptor, which consists of a poly(T) sequence and a sequence complementary to the universal primer used in following qRT-PCR analysis. SNORD44, SNORD47, and SNORD48 were used as internal controls. For qRT-PCR analysis of mRNA expression levels, total RNA was reversely transcribed using

M-MLV Reverse Transcriptase with oligo(dT) 12–18 Primer (Invitrogen). Ribosomal protein L19 (RPL19) was used as internal control. qRT-PCR was performed using SYBR Green PCR Master Mix (Applied Biosystems, Foster City, CA) on StepOnePlus or ViiA 7 Real-Time PCR System (Applied Biosystems). Primer sequences are in the Table S1.

Bromodeoxyuridine cell proliferation assay

Cell proliferation was measured using a bromodeoxyuridine (BrdU) cell proliferation assay kit (EMD Millipore, Billerica, MA).[12] Briefly, mPASMCs were plated into a 96-well plate at a density of 3000 cells/well and incubated overnight. BrdU label was added to the culture medium the next day and cells cultured for another 16–18 h. Colorimetric measurements were carried out on a GloMax 96 Microplate Luminometer (Promega, Madison, WI). For proliferation assay of mPASMCs transfected with miRNA oligos, BrdU label was added 24 h after transfection.

Cell growth curve

PASMCs were plated into 6-well plate at a density of 50,000 cells per well (day 0). On the next day (day 1), PASMCs were infected with Ad-miR212 (100 plaque-forming units [PFUs]/cell) or Ad-Ctrl (100 PFUs/cell). Then cells were collected for cell counting on day 3 and 5, respectively.

Immunofluorescence staining

PASMCs infected with Ad-miR212 or Ad-Ctrl were incubated with 20 ng/mL PDGF-BB for 24 h and then fixed for immunofluorescence staining, as described before.[12] Briefly, cells were fixed with 4% paraformaldehyde (PFA) at room temperature for 15 min and then blocked with blocking buffer (PBS that contains 3% BSA, 1% goat serum, and 0.1% Triton X-100) at room temperature for 30 min. Then cells were incubated with primary antibody (Ki-67, 1:200, Sigma-Aldrich, St. Louis, MO) at 4°C overnight, followed by washing and secondary antibody (1:500, Invitrogen) incubation at room temperature for 30 min. After DAPI staining, cells were imaged with Zeiss LSM 710 Confocal Microscope (Fluorescence Imaging Core, UIC).

miRNA antagonists and mimics

All miRVana miRNA inhibitors and mimics for functional studies were purchased from Ambion, Thermo Fisher Scientific. Negative control miRNA inhibitor #1 or Negative control miRNA mimic #1 was used as the miRNA inhibitor or mimic control, respectively.

Animal studies

All animals were cared for in accordance with the University of Illinois at Chicago animal care policy. Animal experimental protocols were reviewed and approved by the Institutional Animal Care and Use Committee. The 6-8-week-old male C57BL/6 mice were purchased from the Jackson Laboratory (Bar Harbor, ME); 6-7-week-old male Sprague-Dawley rats were purchased from Charles River Laboratories (Cambridge, MA).

Details of each animal study were described below. For i.t. delivery of EVs or adenoviral particles into mice/rats, and right ventricular systolic pressure (RVSP) measurements, animals were first anesthetized with ketamine (100 mg/kg BW) and xylazine (5 mg/kg) via intraperitoneal (i.p.) injection. The anesthetics were given once before each procedure and depth of anesthesia was monitored by toe pinching to determine the loss of reflexes. After RVSP measurement, animals were euthanized under anesthesia followed by lung perfusion/exsanguination.

Assessment of pulmonary hypertension in animal studies

RVSP, Fulton's index, and lung vascular remodeling (pulmonary vessel wall thickness) were used as indices of severity of PH.

In vivo RVSP measurements

To measure RVSP, as a surrogate for pulmonary artery pressure, mice were anesthetized with ketamine/xylazine (100 and 5 mg/kg BW, i.p.) and placed on a heating pad to maintain body temperature. A Millar ultraminiature pressure transducer (1.0 Fr; Millar Instruments, Houston, TX) was introduced into the RV via the jugular vein to obtain pressure measurements.

Measurement of ventricular weights to assess right heart hypertrophy

The RV was dissected from the left ventricle and interventricular septum (LV + S), and the ratios of their weights (RV/[LV + S]) (Fulton's index) was measured and calculated as an index of RV hypertrophy.

Lung vascular morphometry

Lungs were inflated at 20 cm H_2O pressure and fixed with 10% buffered formalin via the trachea. Lungs were also perfused sequentially with PBS and 10% buffered formalin at the same pressure via the RV. Fixed lungs were paraffin-embedded, cut into 5 μm sections, and stained with H&E at the Research Histology and Tissue Imaging Core of UIC. The stained slides were scanned using Aperio ScanScope (Leica Biosystems, Buffalo Grove, IL). Pulmonary arterioles, typically 50–100 μm in diameter for mice and 50–200 μm for rats, adjacent to bronchioles, were measured for wall thickness, represented by the difference between the area of the entire vessel and area of the lumen divided by the area of the entire vessel.

To investigate the role of endogenous miR-212-5p in hypoxia-induced PH, SMC-specific miR-212 knockout mice (sm-212$^{-/-}$) were generated by crossbreeding miR-212 flox/flox mice (provided by Dr. Karl Obrietan at Ohio State University) with SM22a-Cre mouse (Jackson Laboratory). sm-212$^{-/-}$ mice and their 212 fL/fl littermates were exposed to room air or hypoxia (10% O_2, BioSpherix, Parish, NY) for 3 weeks before PH indices were measured.

For miR-212-5p inhibitor study, mice were exposed to room air (normoxia, N) or hypoxia in a hypoxia chamber (10% O_2, H, BioSpherix) and injected with negative control or miR-212-5p inhibitor (Ambion)

via tail vein at a dose of 5 mg/kg BW twice per week. At the end of 2 weeks, mice were sacrificed and PH indices measured.

To investigate if exogenous miR-212-5p can ameliorate hypoxia-induced PH, mice were injected with negative control or miR-212-5p mimic (Ambion) via tail vein at a dose of 5 mg/kg BW twice per week, while they were exposed to room air or hypoxia (10% O_2) for 3 weeks. At the end of 3 weeks, mice were sacrificed and PH indices measured.

To determine if exogenous miR-212-5p can reverse Sugen 5416/hypoxia-induced PH in rats, rats were given one dose of Sugen5416 (20 mg/kg BW, s.c.) and then exposed to hypoxia (H, 10% O_2) for 3 weeks, followed by 2 weeks in room air, to allow severe PH to develop. Then, rats were given 10^8 PFUs control adenoviral particles (Ad-Ctrl) or Ad-miR-212 via trachea, weekly for 3 weeks while they were in room air. Rats given DMSO (Vehicle, Veh) and exposed to room air served as controls. At the end of the study, rats were sacrificed and PH indices measured.

To investigate if eEVs can attenuate/reverse established hypoxia-induced PH in mice, mice were exposed to hypoxia (H, 10% O_2) for 2 weeks to establish PH and then given 5×10^8 Ctrl- or 212-eEVs, i.t., twice a week for 2 weeks while mice were in hypoxia. At the end of 4 week, mice were sacrificed and PH indices measured.

To investigate if eEVs can attenuate/reverse established Sugen 5416/hypoxia-induced severe PH in rats, severe PH was induced in rats using the Sugen/hypoxia protocol described above. Then rats were given 5×10^9 Ctrl- or 212-eEVs, i.t., weekly for 3 weeks while in room air. At the end of study, rats were sacrificed and PH indices measured.

In situ hybridization

MiR-212-5p in the lung was detected using the digoxigenin (DIG) -abeled miRCURY LNA miR-212-5p probe (Qiagen), following an ISH procedure by Deng et al.[9] Briefly, 5 μm lung sections were deparaffinized with xylene and then rehydrated with graded concentration (100%, 96%, 70%, and 50%) of ethanol. Then, slides were boiled for 10 min in diethyl pyrocarbonate (DEPC)-treated 10 mM sodium citrate buffer (pH 6.0). After being washed three times with DEPC-treated PBS, slides were incubated with 0.3% Triton X-100 at room temperature for 10 min, then with freshly made 1× Proteinase K (Qiagen) at 37°C for 15 min, and finally with 4% PFA at room temperature for 15 min. Following incubation with 1× miRCURY LNA miRNA ISH buffer (Qiagen) at 60°C for 1 h, slides were incubated with 40 nM miR-212-5p probe in the same 1× ISH buffer at 60°C overnight. After stringency washing with different concentrations of SSC buffer and blocking, slides were incubated with anti-DIG antibody (1:500, BioChain, Newark, CA) at 4°C overnight. Then, slides were washed and incubated with NBT/BCIP solution (BioChain) in the dark overnight at room temperature. The next day, slides were rinsed with distilled water and dehydrated with graded concentration (50%, 70%, 96%, and 100%) of ethanol and xylene, and then mounted with Shandon Consul-Mount (Thermo Scientific). Staining of miR-212-5p in the lung sections was checked after Aperio whole-slide scanning and using an Aperio ImageScope program.

Statistical analysis

All experiments were repeated at least three times independently. For *in vivo* experiments, at least five animals were used in each group. For isolation of mPASMCs, there were at least three mice in each group. Student's t tests were used when comparing two conditions and a one-way ANOVA with Bonferroni correction was used for multiple comparisons using GraphPad Prism 9 (GraphPad, San Diego, CA) and Microsoft Excel (Microsoft, Redmond, WA), when applicable. Data are presented as mean ± SEM. For significant differences, $p < 0.05$, 0.01, and 0.001 was set. Power of *in vivo* studies was calculated via https://www.stat.ubc.ca/~rollin/stats/ssize/n2.html.

SUPPLEMENTAL INFORMATION

Supplemental information can be found online at https://doi.org/10.1016/j.omtn.2022.06.008.

ACKNOWLEDGMENTS

We thank UIC Electron Microscopy Core, Fluorescence Imaging Core, Research Histology and Tissue Imaging Core (RHTIC), and University of Chicago Integrated Light Microscopy Core for their professional services and assistance for our study. This work is partly supported by an NIH R01HL123804 (J.U.R. and G.Z.), an American Lung Association Biomedical Research Award RG-416135 (T.C.), an American Heart Association Career Development Award 18CDA34110301 (T.C.) and a Gilead Sciences Research Scholars Program in Pulmonary Arterial Hypertension (T.C.), an NIH 1R56-HL141206-01 (J.U.R. and T.C.), a Chicago Biomedical Consortium Catalyst Award (J.U.R., T.C., and J.H.). Bioinformatics analysis in the project described was performed by the UIC Research Informatics Core, supported in part by NCATS through grant UL1TR002003.

AUTHOR CONTRIBUTIONS

T.C. and J.U.R. contributed to the conception and design of the work and interpretation of data; T.C., M.R.S., Q.Z., A.M.G., R.R., J.C., and B.G. conducted the experiments; T.C., M.R.S., D.R.F., B.G., and M.M.-C. contributed to the analysis of data; K.O. contributed to the generation of miR-212 fL/fl mice; T.C. and J.U.R. drafted the work; and M.R.S. also contributed to editing the manuscript.

DECLARATION OF INTERESTS

The authors declare no competing interests.

REFERENCES

1. Humbert, M., Sitbon, O., and Simonneau, G. (2004). Treatment of pulmonary arterial hypertension. N. Engl. J. Med. *351*, 1425–1436. https://doi.org/10.1056/nejmra040291.

2. McLaughlin, V.V., Archer, S.L., Badesch, D.B., Barst, R.J., Farber, H.W., Lindner, J.R., Mathier, M.A., McGoon, M.D., Park, M.H., Rosenson, R.S., et al. (2009). ACCF/AHA 2009 expert consensus document on pulmonary hypertension: a report of the American college of cardiology foundation task force on expert consensus documents and the American heart association: developed in collaboration with the American college of chest physicians, American thoracic society, Inc., and the pulmonary

hypertension association. Circulation *119*, 2250–2294. https://doi.org/10.1161/circulationaha.109.192230.

3. Niwa, R., and Slack, F.J. (2007). The evolution of animal microRNA function. Curr. Opin. Genet. Dev. *17*, 145–150. https://doi.org/10.1016/j.gde.2007.02.004.

4. Williams, A.E. (2008). Functional aspects of animal microRNAs. Cell. Mol. Life Sci. *65*, 545–562. https://doi.org/10.1007/s00018-007-7355-9.

5. Davis-Dusenbery, B.N., and Hata, A. (2010). MicroRNA in cancer: the Involvement of aberrant MicroRNA biogenesis regulatory pathways. Genes Cancer *1*, 1100–1114. https://doi.org/10.1177/1947601910396213.

6. Davis-Dusenbery, B.N., Wu, C., and Hata, A. (2011). Micromanaging vascular smooth muscle cell differentiation and phenotypic modulation. Arterioscler. Thromb. Vasc. Biol. *31*, 2370–2377. https://doi.org/10.1161/atvbaha.111.226670.

7. Babicheva, A., Ayon, R.J., Zhao, T., Ek Vitorin, J.F., Pohl, N.M., Yamamura, A., Yamamura, H., Quinton, B.A., Ba, M., Wu, L., et al. (2020). MicroRNA-mediated downregulation of K(+) channels in pulmonary arterial hypertension. Am. J. Physiol. Lung Cell Mol. Physiol. *318*, L10–L26. https://doi.org/10.1152/ajplung.00010.2019.

8. Caruso, P., Dempsie, Y., Stevens, H.C., McDonald, R.A., Long, L., Lu, R., White, K., Mair, K.M., McClure, J.D., Southwood, M., et al. (2012). A role for miR-145 in pulmonary arterial hypertension: evidence from mouse models and patient samples. Circ. Res. *111*, 290–300. https://doi.org/10.1161/circresaha.112.267591.

9. Deng, L., Blanco, F.J., Stevens, H., Lu, R., Caudrillier, A., McBride, M., McClure, J.D., Grant, J., Thomas, M., Frid, M., et al. (2015). MicroRNA-143 activation regulates smooth muscle and endothelial cell crosstalk in pulmonary arterial hypertension. Circ. Res. *117*, 870–883. https://doi.org/10.1161/circresaha.115.306806.

10. Mondejar-Parreño, G., Callejo, M., Barreira, B., Morales-Cano, D., Esquivel-Ruiz, S., Moreno, L., Cogolludo, A., and Perez-Vizcaino, F. (2019). miR-1 is increased in pulmonary hypertension and downregulates Kv1.5 channels in rat pulmonary arteries. J. Physiol. *597*, 1185–1197. https://doi.org/10.1113/jp276054.

11. Ruffenach, G., Chabot, S., Tanguay, V.F., Courboulin, A., Boucherat, O., Potus, F., Meloche, J., Pflieger, A., Breuils-Bonnet, S., Nadeau, V., et al. (2016). Role for runt-related transcription factor 2 in proliferative and calcified vascular lesions in pulmonary arterial hypertension. Am. J. Respir. Crit. Care Med. *194*, 1273–1285. https://doi.org/10.1164/rccm.201512-2380oc.

12. Chen, T., Zhou, G., Zhou, Q., Tang, H., Ibe, J.C.F., Cheng, H., Gou, D., Chen, J., Yuan, J.X.J., and Raj, J.U. (2015). Loss of MicroRNA-17-92 in smooth muscle cells attenuates experimental pulmonary hypertension via induction of PDZ and LIM domain 5. Am. J. Respir. Crit. Care Med. *191*, 678–692. https://doi.org/10.1164/rccm.201405-0941oc.

13. Chen, T., Sun, M.R., Zhou, Q., Guzman, A.M., Ramchandran, R., Chen, J., Ganesh, B., and Raj, J.U. (2022). Extracellular vesicles derived from endothelial cells in hypoxia contribute to pulmonary artery smooth muscle cell proliferation in-vitro and pulmonary hypertension in mice. Pulm. Circ. *12*, e12014. https://doi.org/10.1002/pul2.12014.

14. Abels, E.R., and Breakefield, X.O. (2016). Introduction to extracellular vesicles: biogenesis, RNA cargo selection, content, release, and uptake. Cell. Mol. Neurobiol. *36*, 301–312. https://doi.org/10.1007/s10571-016-0366-z.

15. Deatherage, B.L., and Cookson, B.T. (2012). Membrane vesicle release in bacteria, eukaryotes, and archaea: a conserved yet underappreciated aspect of microbial life. Infect. Immun. *80*, 1948–1957. https://doi.org/10.1128/iai.06014-11.

16. Saari, H., Lázaro-Ibáñez, E., Viitala, T., Vuorimaa-Laukkanen, E., Siljander, P., and Yliperttula, M. (2015). Microvesicle- and exosome-mediated drug delivery enhances the cytotoxicity of Paclitaxel in autologous prostate cancer cells. J. Control. Release *220*, 727–737. https://doi.org/10.1016/j.jconrel.2015.09.031.

17. Kamerkar, S., LeBleu, V.S., Sugimoto, H., Yang, S., Ruivo, C.F., Melo, S.A., Lee, J.J., and Kalluri, R. (2017). Exosomes facilitate therapeutic targeting of oncogenic KRAS in pancreatic cancer. Nature *546*, 498–503. https://doi.org/10.1038/nature22341.

18. Arenaccio, C., Chiozzini, C., Ferrantelli, F., Leone, P., Olivetta, E., and Federico, M. (2018). Exosomes in therapy: engineering, pharmacokinetic, and future applications. Curr. Drug Targets *19*.

19. Mendt, M., Kamerkar, S., Sugimoto, H., McAndrews, K.M., Wu, C.C., Gagea, M., Yang, S., Blanko, E.V.R., Peng, Q., Ma, X., et al. (2018). Generation and testing of clinical-grade exosomes for pancreatic cancer. JCI Insight *3*, 99263. https://doi.org/10.1172/jci.insight.99263.

20. Mentkowski, K.I., Snitzer, J.D., Rusnak, S., and Lang, J.K. (2018). Therapeutic potential of engineered extracellular vesicles. AAPS J. *20*, 50. https://doi.org/10.1208/s12248-018-0211-z.

21. Tian, T., Zhang, H.X., He, C.P., Fan, S., Zhu, Y.L., Qi, C., Huang, N.P., Xiao, Z.D., Lu, Z.H., Tannous, B.A., and Gao, J. (2018). Surface functionalized exosomes as targeted drug delivery vehicles for cerebral ischemia therapy. Biomaterials *150*, 137–149. https://doi.org/10.1016/j.biomaterials.2017.10.012.

22. Ye, Z., Zhang, T., He, W., Jin, H., Liu, C., Yang, Z., and Ren, J. (2018). Methotrexate-loaded extracellular vesicles functionalized with therapeutic and targeted peptides for the treatment of glioblastoma multiforme. ACS Appl. Mater. Interfaces *10*, 12341–12350. https://doi.org/10.1021/acsami.7b18135.

23. Remenyi, J., van den Bosch, M.W.M., Palygin, O., Mistry, R.B., McKenzie, C., Macdonald, A., Hutvagner, G., Arthur, J.S.C., Frenguelli, B.G., and Pankratov, Y. (2013). miR-132/212 knockout mice reveal roles for these miRNAs in regulating cortical synaptic transmission and plasticity. PLoS One *8*, e62509. https://doi.org/10.1371/journal.pone.0062509.

24. Hansen, K.F., Sakamoto, K., Aten, S., Price, K.H., Loeser, J., Hesse, A.M., Page, C.E., Pelz, C., Arthur, J.S.C., Impey, S., and Obrietan, K. (2016). Targeted deletion of miR-132/-212 impairs memory and alters the hippocampal transcriptome. Learn. Mem. *23*, 61–71. https://doi.org/10.1101/lm.039578.115.

25. Faught, E., Henrickson, L., and Vijayan, M.M. (2017). Plasma exosomes are enriched in Hsp70 and modulated by stress and cortisol in rainbow trout. J. Endocrinol. *232*, 237–246. https://doi.org/10.1530/joe-16-0427.

26. Mathew, B., Ravindran, S., Liu, X., Torres, L., Chennakesavalu, M., Huang, C.C., Feng, L., Zelka, R., Lopez, J., Sharma, M., and Roth, S. (2019). Mesenchymal stem cell-derived extracellular vesicles and retinal ischemia-reperfusion. Biomaterials *197*, 146–160. https://doi.org/10.1016/j.biomaterials.2019.01.016.

27. Chen, W., Bian, H., Xie, X., Yang, X., Bi, B., Li, C., Zhang, Y., Zhu, Q., Song, J., Qin, C., and Qi, J. (2020). Negative feedback loop of ERK/CREB/miR-212-3p inhibits HBeAg-induced macrophage activation. J. Cell Mol. Med. *24*, 10935–10945. https://doi.org/10.1111/jcmm.15723.

28. Remenyi, J., Hunter, C.J., Cole, C., Ando, H., Impey, S., Monk, C.E., Martin, K.J., Barton, G.J., Hutvagner, G., and Arthur, J.S. (2010). Regulation of the miR-212/132 locus by MSK1 and CREB in response to neurotrophins. Biochem. J. *428*, 281–291. https://doi.org/10.1042/bj20100024.

29. Yue, H., Liu, L., and Song, Z. (2019). miR-212 regulated by HIF-1α promotes the progression of pancreatic cancer. Exp. Ther. Med. *17*, 2359–2365. https://doi.org/10.3892/etm.2019.7213.

30. Malm, H.A., Mollet, I.G., Berggreen, C., Orho-Melander, M., Esguerra, J.L.S., Göransson, O., and Eliasson, L. (2016). Transcriptional regulation of the miR-212/miR-132 cluster in insulin-secreting beta-cells by cAMP-regulated transcriptional co-activator 1 and salt-inducible kinases. Mol. Cell. Endocrinol. *424*, 23–33. https://doi.org/10.1016/j.mce.2016.01.010.

31. Jones, C., Bisserier, M., Bueno-Beti, C., Bonnet, G., Neves-Zaph, S., Lee, S.Y., Milara, J., Dorfmüller, P., Humbert, M., Leopold, J.A., et al. (2020). A novel secreted-cAMP pathway inhibits pulmonary hypertension via a feed-forward mechanism. Cardiovasc. Res. *116*, 1500–1513. https://doi.org/10.1093/cvr/cvz244.

32. Garat, C.V., Majka, S.M., Sullivan, T.M., Crossno, J.T., Jr., Reusch, J.E.B., and Klemm, D.J. (2020). CREB depletion in smooth muscle cells promotes medial thickening, adventitial fibrosis and elicits pulmonary hypertension. Pulm. Circ. *10*. https://doi.org/10.1177/2045894019898374.

33. Andaloussi, S.E.L., Mäger, I., Breakefield, X.O., and Wood, M.J.A. (2013). Extracellular vesicles: biology and emerging therapeutic opportunities. Nat. Rev. Drug Discov. *12*, 347–357. https://doi.org/10.1038/nrd3978.

34. Aliotta, J.M., Pereira, M., Wen, S., Dooner, M.S., Del Tatto, M., Papa, E., Goldberg, L.R., Baird, G.L., Ventetuolo, C.E., Quesenberry, P.J., and Klinger, J.R. (2016). Exosomes induce and reverse monocrotaline-induced pulmonary hypertension in mice. Cardiovasc. Res. *110*, 319–330. https://doi.org/10.1093/cvr/cvw054.

35. Lee, C., Mitsialis, S.A., Aslam, M., Vitali, S.H., Vergadi, E., Konstantinou, G., Sdrimas, K., Fernandez-Gonzalez, A., and Kourembanas, S. (2012). Exosomes mediate the cytoprotective action of mesenchymal stromal cells on hypoxia-induced pulmonary

hypertension. Circulation *126*, 2601–2611. https://doi.org/10.1161/circulationaha.112.114173.

36. Bhome, R., Del Vecchio, F., Lee, G.H., Bullock, M.D., Primrose, J.N., Sayan, A.E., and Mirnezami, A.H. (2018). Exosomal microRNAs (exomiRs): small molecules with a big role in cancer. Cancer Lett. *420*, 228–235. https://doi.org/10.1016/j.canlet.2018.02.002.

37. Villarroya-Beltri, C., Gutiérrez-Vázquez, C., Sánchez-Cabo, F., Pérez-Hernández, D., Vázquez, J., Martin-Cofreces, N., Martinez-Herrera, D.J., Pascual-Montano, A., Mittelbrunn, M., and Sánchez-Madrid, F. (2013). Sumoylated hnRNPA2B1 controls the sorting of miRNAs into exosomes through binding to specific motifs. Nat. Commun. *4*, 2980. https://doi.org/10.1038/ncomms3980.

38. Hergenreider, E., Heydt, S., Tréguer, K., Boettger, T., Horrevoets, A.J.G., Zeiher, A.M., Scheffer, M.P., Frangakis, A.S., Yin, X., Mayr, M., et al. (2012). Atheroprotective communication between endothelial cells and smooth muscle cells through miRNAs. Nat. Cell Biol. *14*, 249–256. https://doi.org/10.1038/ncb2441.

39. Prokopi, M., Pula, G., Mayr, U., Devue, C., Gallagher, J., Xiao, Q., Boulanger, C.M., Westwood, N., Urbich, C., Willeit, J., et al. (2009). Proteomic analysis reveals presence of platelet microparticles in endothelial progenitor cell cultures. Blood *114*, 723–732. https://doi.org/10.1182/blood-2009-02-205930.

40. György, B., Szabó, T.G., Turiák, L., Wright, M., Herczeg, P., Lédeczi, Z., Kittel, Á., Polgár, A., Tóth, K., Dérfalvi, B., et al. (2012). Improved flow cytometric assessment reveals distinct microvesicle (cell-derived microparticle) signatures in joint diseases. PLoS One *7*, e49726. https://doi.org/10.1371/journal.pone.0049726.

41. Sódar, B.W., Kittel, Á., Pálóczi, K., Vukman, K.V., Osteikoetxea, X., Szabó-Taylor, K., Németh, A., Sperlágh, B., Baranyai, T., Giricz, Z., et al. (2016). Low-density lipoprotein mimics blood plasma-derived exosomes and microvesicles during isolation and detection. Sci. Rep. *6*, 24316. https://doi.org/10.1038/srep24316.